Induced polarization effects in frequency domain AEM data

D.Khliustov[1], E.Karshakov[2]
1. Institute of Control Sciences
Russia, hlustov.d@gmail.com
2. Institute of Control Sciences
Russia, karshakov@ipu.ru

BIOGRAPHY

E. Karshakov is the CEO of Geotechnologies Inc. and head of a laboratory in V. A. Trapeznikov Institute of Control Sciences.
D. Khliustov is an engineer in Geotechnologies Inc. and junior researcher in V. A. Trapeznikov Institute of Control Sciences.

SUMMARY

Induced polarization (IP) effects may have significant impact on airborne electromagnetic (AEM) data. They manifest themselves in dependence of apparent resistivity on the frequency of the signal. Usually in order to model IP one derives analytical formulas describing the dependence of resistivity on frequency for each layer of the model. However, the number of parameters thus grows fast with the number of layers included in the model. Hence the inversion of data becomes an ill posed problem.

This work suggests an approach to overcoming this difficulty. We show that the effects of IP are concentrated in relatively small number of layers and propose a simple algorithm for finding them. The results of inverting real data showing strong IP are presented.

Key words: data inversion, airborne electromagnetics, induced polarization.

INTRODUCTION

The effect of induced polarisation (IP) has been a subject of discussion in the field of airborne electromagnetics (AEM) data processing for a long time (Kaminski and Viezzoli, 2016). The reason for it is that for many real data the IP not taken into account leads to inconsistent results of inversion, e. g., acute contrast in resistivities of consecutive layers.

It should be noted that sometimes IP is only visible if frequency spectrum of AEM system is sufficiently dense, and the flight altitude is low. Figure 1 provides inversion results for AEM system EQUATOR, taking measurements of 25 frequencies ranging from 77 Hz to 15000 Hz, and four frequency system EM4H in fixed wing (high altitude) and helicopter (low altitude) configurations. The survey has been conducted in Norilsk region, where IP is widely present due to permafrost and ice melting.

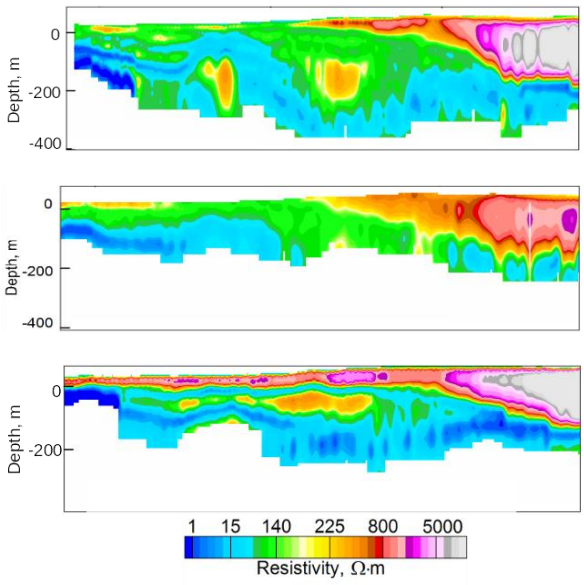

Figure 1. Inversion results for EQUATOR system and two configurations of EM4H system

It can be noticed the contrasts in the right part of figure, which may be attributed to IP, are sharp for EQUATOR, significant for helicopter EM4H and quite mild for fixed wing system.

One of the possible indicators of IP are negative values of time domain response or in-phase component of spectral response (Karshakov and Moilanen, 2019). The mathematical equivalence between these is an open problem.

Possible explanations of IP effect are numerous. One point of view is that it should be attributed to properties of conductive medium. There are works devoted to construction of materials with inductive properties, capable of conserving electric charge (Gurin et al., 2019). The laboratory experiments suggest that in the presence of inhomogeneity (such as contrast of resistivity or porosity) the medium may show frequency-dependent conductivity.

Another point of view is that IP effects are caused by geometric properties of the environment. Complex relief or presence of surface cracks may lead to medium behavior similar to that of capacitor, or, more generally, Warburg element.

The first part of the current work is devoted to the study of well-known Cole-Cole model. It is shown that the original formula has to be modified in order to produce results consistent with phenomenological indicators of IP presence. After this an inversion methodology is suggested which helps to reduce the number of

parameters and thus make the problem better conditioned.

In all the computations made below parameters of the AEM system (frequencies, typical altitudes, relative position of emitter and receiver) correspond to those of EQUATOR (Moilanen et al., 2013).

METHOD AND RESULTS

Model formulation

When computing resistivity structure of a medium explaining real data it is a common choice to use horizontally layered model (Zhdanov, 2009). This simplification leads to reduced amount of computations while providing good explanatory power. In this model the response to the field of vertical magnetic dipole is derived explicitly. Namely, for a given frequency ω the vertical component of the response is

$$H_z(\omega) = \int_0^\infty u(n_0, z, h_T, \omega) J_0(n_0 r) n_0^2 dn_0, \quad (1)$$

where J_0 is the zero-order Bessel function of the first kind, r is the horizontal shift of the receiver with respect to the dipole axis, h_T is the altitude of the dipole above the ground, z is the altitude of the receiver. Here u is the two-dimensional spectrum of the potential of the secondary field:

$$u(n_0, z, h_T, \omega) = \frac{M exp(-n_0(z+h))}{2} \frac{n_1 - n_0 R^0}{n_1 + n_0 R^0}, \quad (2)$$

where M is the amplitude of the dipole moment and R^0 is the reduced spectral impedance of the medium. For K layers it is given by the formula

$$R^0 = tanh\left(n_1 h_1 + \cdots tanh^{-1}\left(n_{K-1} h_{K-1} + tanh^{-1}\frac{n_{K-1}}{n_K}\right)\right), \quad (3)$$

where

$$n_k = \sqrt{n_0^2 - \frac{i\omega\mu_0}{\rho_k}}, Re\, n_k > 0. \quad (4)$$

In the above formula $\mu_0 = 4\pi \times 10^{-7}$ H/m is the magnetic permittivity, ρ_k is the resistivity of k'th layer.

One of the possible approaches to solving the inverse problem (estimating resistivities and thicknesses of the layers from data) is the Kalman filter. The presence of non-linearities advocates the use of variants of Kalman approach, such as Extended and Iterated filters (Karshakov, 2020). The non-linearity also leads to solution being dependent on initial conditions used in the algorithm.

The above formulas are direct consequences of Maxwell equations. Since all computations are produced in spectral domain, there is nothing prohibiting one from use of frequency dependent resistivities. The corresponding time domain solution in this case can be found by inverse Fourier transform (possibly discrete).

The effect of IP is usually modelled by introducing resistivity of a special form, governed by Cole-Cole equations (Cole and Cole, 1941, Pelton et al., 1978):

$$\rho = \rho_0\left(1 - m\left(1 - \frac{1}{1+(i\omega\tau)^c}\right)\right), \quad (5)$$

where ρ_0 is DC current resistivity, m is chargeability constant, τ is a relaxation time, c is a phase constant. These equations were originally introduced for so-called slow IP, connected to movement of charged particles in electrolite. However, they were later applied to AEM data processing on empirical basis. Other resistivity models of this kind exist in literature (see Dias, 2000), but they usually include more parameters, which makes inverse problem even worse posed.

Another thing to notice is that the function $(i\omega\tau)^c$ has several branches, and hence we must choose among a set of possible values. Indeed, $i = exp\left(\frac{i*\pi}{2}\right) = exp\left(i * \left(\frac{\pi}{2} + 2\pi k\right)\right)$ for an integer k. Hence after raising it to the power of c we obtain $exp\left(i\frac{c\pi}{2}\right)$, $exp\left(i\frac{5c\pi}{2}\right)$, ... as possible values, all distinct as soon as c and π are incommensurable. We further remark on this issue in the next section.

Theoretical considerations

As it was already mentioned, one of the main practical indicators of IP is the presence of negative in-phase response in the spectral data. We tried to obtain it in simulation by posing optimization problem $Re\, H_z(\omega) \to min$ and solving it over ω and resistivity parameters. It turned out that in order for the problem to have negative solution one must have $Re\, \rho_k > 0$, $Im\, \rho_k > 0$ for resistivity of at least one of the layers. However, the original Cole-Cole model corresponding to the first branch of power function is uncapable of producing such resistivity. Hence we have chosen another branch of the function, taking $i^c = exp\left(i\frac{5c\pi}{2}\right)$. The results of simulating half-space model with parameters $\rho = 1000\,\Omega \cdot m$, $m = 0.5$, $\tau = 0.001$ s, $c = 0.5$ are presented in figure 2. There we present three curves for each graph: quadrature (Im) and inphase (Re) components in frequency domain and off-time signal in time-domain. Index "IP0" is related to the branch number 0 , "IP1" is related to the branch number 1 , "noIP" is related to non-polarizable medium.

However, it is not clear why we should choose this branch of power function instead of any other. One of the possible approaches would be to introduce additional phase parameter in Cole-Cole formula and search for branch of the form $exp(i\psi)$. But this leads to functions with singularities in the domain and is a subject of further investigation.

If the model has all resistivities determined by Cole-Cole formula, the number of parameters is high. Hence one needs an additional regularization in order for the inverse problem to be tractable. We adopted a hypothesis that chargeability is determined by relatively small number of layers (1-3). To find these layers, we fitted a model with one chargeable layer and non-chargeable others. After varying the depth in which chargeability was located, we could obtain residuals between model prediction and measured response. For some depths, the residual turned out to be several times lower (30-40 as compared to 150-200) than for others. Although it was still too high to consider any of obtained result a good fit, this procedure enabled us to make a choice as to which layers should be chargeable.

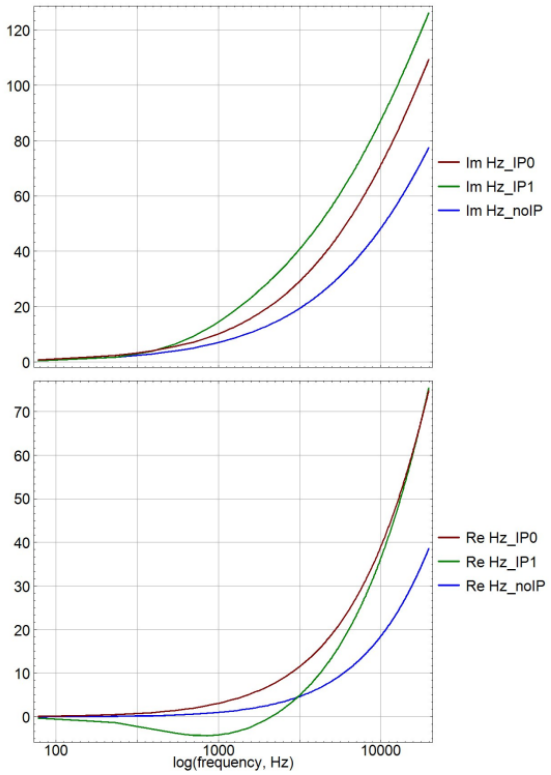

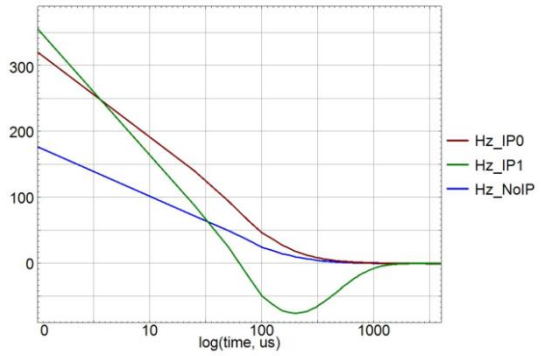

Figure 2. The response of half-space model in frequency (quadrature and inphase) and time domains

This simple algorithm is valid only for small sections of data, since the actual profile can change significantly on large scales. When the residual of final model becomes too high, one needs to repeat the procedure and determine new depths of chargeable layers.

Main results

Here we provide results of real data processing based on our approach. The data consisted of responses for 15 frequencies ranging from 77 to 15000 Hz, with in-phase and quadrature components measured for each. We used model with 25 layers with thickness of i'th layer equal to $4 * 1.1085^i$ meters. The first step of the algorithm consisted in fitting the model which had frequency dependent resistivity in one of 25 layers. An example of relative discrepancy determined by formula

$$\left(\sum_{\omega_i} \frac{(response_{estimated}(\omega_i) - response_{true}(\omega_i))^2}{\sigma^2_{noise}(\omega_i)}\right)^{\frac{1}{2}} \quad (6)$$

where response consists of in-phase and quadrature components for each frequency, is presented in figure 3.

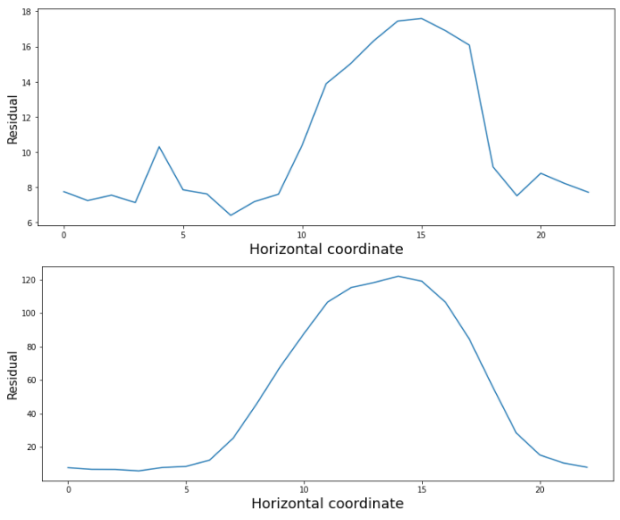

Figure 3. The residual of model with one chargeable layer
(top) Chargeability in layer # 2
(bottom) Chargeability in layer # 5
The second graph clearly exceeds the first

It is easy to see that by locating chargeability in layer #2 we decrease residual significantly compared to locating it in layer #5.

It turned out that in order to decrease the residual one must locate chargeability in layers 2, 4, 6 and 7. In order to further decrease the number of parameters we changed consecutive layers 6 and 7 to one layer with thickness equal to the sum of respective thicknesses. Hence we had to fit a model with 33 parameters. The resulting relative discrepancy is given in figure 4. It is easy to see that residual does not exceed 10, which may be considered a good fit.

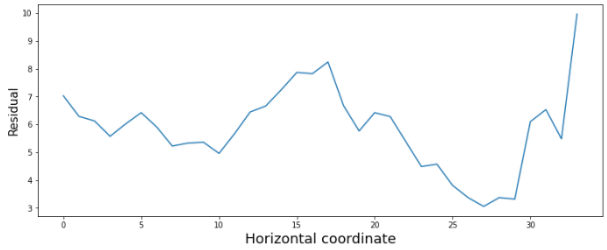

Figure 4. The residual of the final model

Figure 5 gives values of Cole-Cole parameters for each of the layers obtained by model.

Figure 6 shows the results of data inversion. The survey was carried out in Siberia, in the permafrost region. The melting zone is considered to be the main source of chargeability. We would like to point out the following features. First, after applying the chargeable model for the inversion, we see horizontally continuous layers. Second, even in the case of positive in-phase responses (left part), the chargeability model provides more adequate solution according to known local geological properties: the lower conductive layer is presented along the whole flight trajectory.

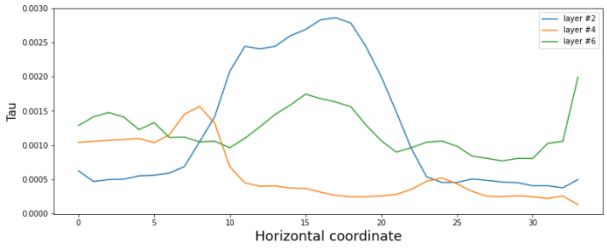

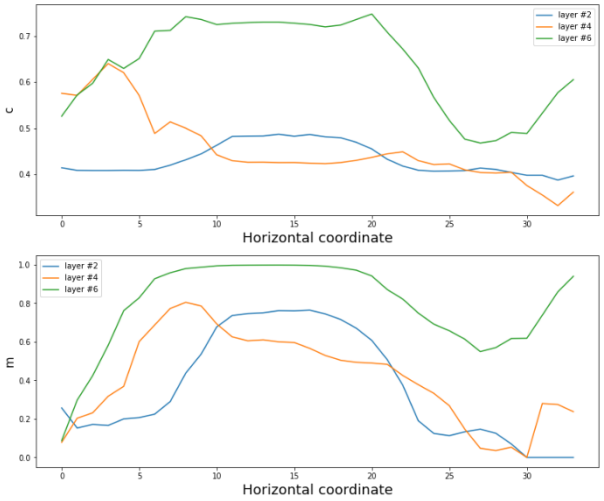

Figure 5. The Cole-Cole parameters: time constant, exponent and chargeability

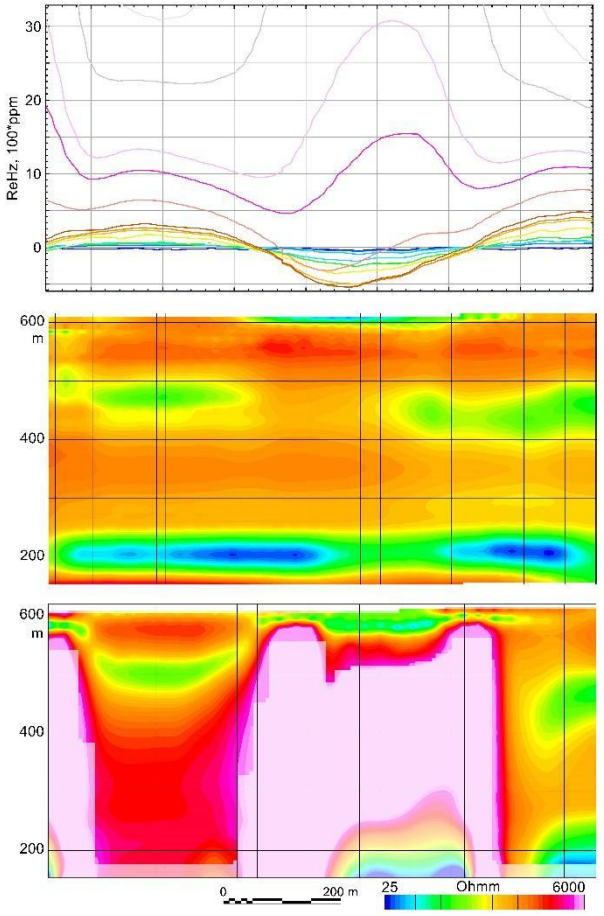

Figure 6. The inphase response curves and inversion results for the models with (top) and without (bottom) chargeability.

CONCLUSIONS

In this work we studied the problem of inverting AEM data in the presence of IP effects. We considered horizontally layered one dimensional model with

frequency dependent resistivity, given by Cole-Cole formula. It has been shown that IP effects are mostly determined by local properties of environment and are concentrated in a small number of layers. Based on this, we suggested an approach to choosing the depth of chargeable layers by fitting several simpler models and analysing residuals.

For a demonstration of our approach, we analysed real data by estimating parameters of our model. We used dataset obtained by the EQUATOR AEM system. The environment demonstrates signs of IP presence, most likely connected to ice melting.

Further research directions include formalizing the procedure of chargeable layer identification. Some additional investigation should be conducted on choosing the appropriate branch of complex-valued resistivity function, discussed above.

REFERENCES

Cole, K.S., and R.H. Cole, 1941. Dispersion and absorption in dielectrics I. Alternating current characteristics. *The Journal of chemical physics* 9(4): 341-351.

Dias, C., 2000. Developments in a model to describe low-frequency electrical polarization of rocks. *Geophysics* 65(2): 437-451.

Gurin, G., Titov, K., and Y. Ilyin, 2019. Induced polarization of rocks containing metallic particles: evidence of passivation effect. *Geophysical Research Letters* 46(2): 670-677.

Kaminski, V., and A. Viezzoli, 2017. Modeling induced polarization effects in helicopter time-domain electromagnetic data: Field case studies. *Geophysics* 82(2): B49-B61.

Karshakov, E., and J. Moilanen, 2019. Overcoming Airborne IP in Frequency Domain: Hopes and Disappointments. *SAGA Biennial Conference & Exhibition*: 1-4.

Karshakov, E., 2020. Iterated extended Kalman filter for airborne electromagnetic data inversion. *Exploration Geophysics* 51(1): 66-73.

Moilanen, J., Karshakov, E., and A. Volkovitsky, 2013. Time-domain helicopter EM System “Equator”: resolution, sensitivity, universality. *13th SAGA biennial and 6thInternational AEM conference AEM-2013*, Expanded Abstracts: 1-4.

Pelton, W.H., Ward, S.H., Hallof, G., Sill, W.R., and P.H. Nelson, 1978. Mineral discrimination and removal of inductive coupling with multifrequency IP. *Geophysics* 43(3): 588-609.

Zhdanov, M. S., 2009. Geophysical electromagnetic theory and methods. Elsevier.